Design of Dual-Band Double Negative Metamaterials

Davoud Zarifi, Seyed Ehsan Hosseininejad, and Ali Abdolali*

Antenna and Microwave Research Laboratory, School of Electrical engineering,
Iran University of Science and Technology

Abstract

A dual-band artificial magnetic material and then a dual-band double-negative metamaterial structure based on symmetric spiral resonators are presented. An approximate analytical model is used for the initial design of the proposed structures. The electromagnetic parameters of the proposed metamaterial structure retrieved using an advanced parameter retrieval method based on the causality principle show its dual-band nature at microwave frequencies.

Keywords: Artificial magnetic materials, Double negative metamaterials, Dual-band structures

1. Introduction

The artificial materials have been the subject of great interest for many worldwide research groups and scientists over the years. Recently, a new class of artificial materials, the so-called metamaterials (MTMs), has been studied extensively owing to its peculiar physical properties and novel applications, which do not occur or might not be readily realizable in nature. The most interesting physical phenomenon of MTMs is the negative refractive index (NRI) [1]. The first implementation of NRI was reported in Smith's experiments using a composite structure, consisting of Split Ring Resonators (SRRs) and continuous wires [2]. Afterwards, while the negative permittivity is still simply obtained from continuous wires, various types of artificial magnetic structures, such as cut-wire pair, H-shaped and π-shaped configurations have been introduced [3-5]. Negative refraction and, in general, electromagnetic wave propagation in NRI media are still controversial subjects and have generated many intense debates. Based on the interesting and unique properties of MTMs, many applications have been proposed for them, such as antennas [6-11], superlenses [12, 13], filters [14-16], and other devices [17-21]. More recently, chiral MTMs have been introduced as an alternative route for achieving NRI media [22-26].

In this study, a dual-band artificial magnetic material and MTM structures are proposed, using symmetric spiral resonators. Briefly, in Sec. 2, the analytical and numerical analysis of dual-band artificial magnetic materials are presented. In Sec. III the application of proposed structure for designing double-negative MTMs is introduced. Finally, summary and conclusions are provided in Sec. 4.

The most significant advantage of the proposed dual-band MTM structure in this study is that its dimensions are similar to the well-known single-band MTM structures [27]. However, the common techniques of realizing dual-band MTMs such as combination of unit cells with different transverse dimensions [28, 29] and using multilayer printed circuit boards [30] causing enlargement of the unit cell dimensions, are totally avoided.

* abdolali@iust.ac.ir

2. Dual-band artificial magnetic material using symmetric spiral resonators

Figure 1 illustrates the unit cell of proposed dual-band artificial magnetic structure. The unit cell with transverse dimensions of 2.5 mm × 2.5 mm, consisting of two symmetric spiral resonators, with width w = 0.1 mm and thickness t = 0.018 mm and other geometric parameters s = 0.05 mm, l_1 = 1.15 mm, l_2 = 1.05 mm, l_3 = 2.4 mm, and l_4 = 2.3 mm were patterned on one side of an FR-4 dielectric board with the dielectric constant ε_r = 4.4, dielectric loss tangent tan δ = 0.025, and thickness h = 0.25 mm. Note that the use of two symmetric spiral resonators is to achieve a dual-band structure.

The analytic model of single-band artificial magnetic material structures were in [31, 32]. We may now study the behaviour of the proposed dual-band magnetic material structure. Observe that when the structure is exposed to an external magnetic field (according to Faraday's Law) the change in the magnetic flux enclosed by the resonators induces an electromotive force in the square copper rings resulting a current in them. Thus, the induced current and resultant magnetic dipole moment is the source of the effective permeability of the structure. It is clear that due to alignment of resonators in the *x*-*y* plane, the resultant effective permeability is generated only in the *z* direction. If only the upper symmetric spiral resonator exists, the effective relative permeability of the structure is given by [32]:

$$\mu_r = 1 - \frac{j\omega L_{eff} A}{d_x d_y \left(R_{ohmic} + \dfrac{1}{G_{eff} + j\omega C_{eff}} + j\omega L_{eff} \right)} \tag{1}$$

where A and ω are the area enclosed by the resonator and the angular frequency, respectively. In addition, L_{eff} is the effective inductance of resonator given by:

$$L_{eff} = \mu_0 \frac{A}{d_z} \tag{2}$$

and C_{eff} is the total effective capacitance of the resonator's strips. The per-unit-length capacitance of the symmetric coplanar strip lines using conformal mapping technique can be expressed as [33]:

$$C_{pul} = \varepsilon_0 \varepsilon_{eff} \frac{K(\sqrt{1-k^2})}{K(k)}, \quad K(k) = \int_0^{\frac{\pi}{2}} \frac{d\phi}{\sqrt{1-k^2 \sin^2 \phi}} \tag{3}$$

$$\varepsilon_{eff} = 1 + \frac{\varepsilon_r - 1}{2} \frac{K(k_1) K(\sqrt{1-k^2})}{K(k) K(\sqrt{1-k_1^2})}, \quad k = \frac{s}{s+2w}, \quad k_1 = \frac{\sinh(\pi s/4h)}{\sinh[\pi(s+2w)/4h]} \tag{4}$$

where ε_{eff} and K are the effective relative permittivity and complete elliptic integral of the first kind, respectively. In order to compute the total capacitance of the resonator's strips, the per-unit-length capacitance of coplanar strips, C_{pul} should be multiplied by the average length of adjacent strips, l_{av}. In addition, R_{ohmic} and G_{eff} corresponding to the ohmic loss of copper strips (σ = 5.8*e*7 S/m), and the loss of substrate, respectively are given by:

$$R_{ohmic} = \frac{l_t}{w} \sqrt{\frac{\omega \mu_0}{2\sigma}}, \quad G_{eff} = \omega \varepsilon_0 \varepsilon_{eff} l_{av} \tan\delta \frac{K(\sqrt{1-k^2})}{K(k)} \tag{5}$$

which l_t is the total length of copper strips of the resonator.

The unit cell of proposed dual-band artificial magnetic structure is now considered. Two symmetric spiral resonators with different dimensions generate two distinct resonant frequencies, between which there is clearly no magnetic coupling. By neglecting the effect of electric coupling between resonators, the effective relative permeability of this configuration can be expressed by:

$$\mu_r = 1 - \frac{j\omega L_{eff}^{(1)} A^{(1)}}{d_x d_y \left(R_{ohmic}^{(1)} + \dfrac{1}{G_{eff}^{(1)} + j\omega C_{eff}^{(1)}} + j\omega L_{eff}^{(1)} \right)} - \frac{j\omega L_{eff}^{(2)} A^{(2)}}{d_x d_y \left(R_{ohmic}^{(2)} + \dfrac{1}{G_{eff}^{(2)} + j\omega C_{eff}^{(2)}} + j\omega L_{eff}^{(2)} \right)} \tag{6}$$

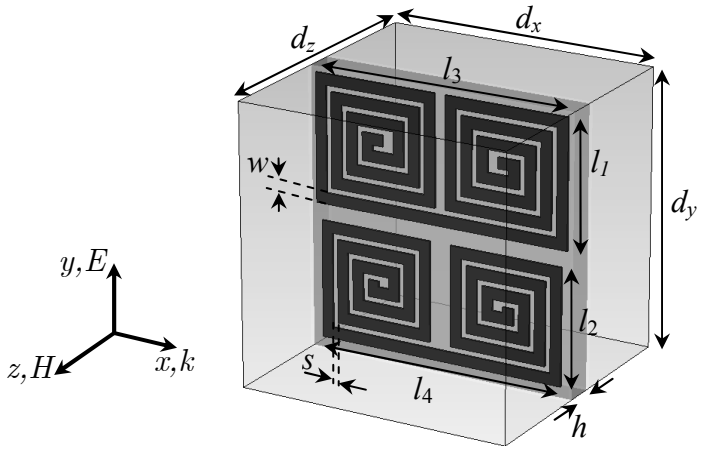

Figure 1. Schematic diagram of the proposed dual-band magnetic structure unit cell. The geometric parameters of the unit cell are given by $d_x = d_y = d_z = 2.5$ mm, $w = 0.1$ mm, $s = 0.05$ mm, $l_1 = 1.15$ mm, $l_2 = 1.05$ mm, $l_3 = 2.4$ mm, $l_4 = 2.3$ mm, and $h = 0.25$ mm.

where (1) and (2) superscripts correspond to the upper and lower resonators, respectively. Due to the considerable width of strips and many corners in the structure, considering of the exact values of effective area enclosed by each resonator, total length of each resonator and the average length of adjacent strips is almost impossible. It can be seen that the effective area enclosed by each resonator, total length of each resonator and the average length of adjacent strips in each resonator are approximately given by:

$$A^{(i)} = \sum_{k=1}^{N} \left[l_i - (2k)w - 2(k-1)s \right]^2 \tag{7}$$

$$l_t^{(i)} = (4N) l_i - (2N)^2 w - (2N-1)^2 s \tag{8}$$

$$l_{av}^{(i)} = 4(N-1) l_i - 4N(N-1)w - 4(N-1)^2 s \tag{9}$$

where i may be set equal to 1 or 2, and $N \geq 2$ is the number of turns of each square spiral structure in a symmetric spiral resonator.

In general, for compact structures, where the space between non-adjacent strips is comparable to the space between adjacent strips, the presented model gives an approximate value for the relative permeability, which can be used to initiate a design. However, we can, once again, perform a more accurate analysis by using a commercial electromagnetic simulator to accurately compute the exact value of the resonance frequencies and the relative permeability of the proposed structure. However this procedure would only provide some fine adjustment.

The resonance frequencies of the proposed symmetric spiral resonators and the resultant structure using the proposed analytical model are calculated and reported in Table 1. Observe that the resonance frequencies of the complete resultant structure are close to those of each resonator. The small shift between them is mainly due to the electric coupling among the resonators.

In order to evaluate the presented analytical model, a full-wave analysis is required. Numerical simulations are performed by using time domain analysis of CST Microwave Studio. The resonance frequencies obtained from simulation are also presented in Table 1. Due to the aforementioned approximations, exact agreement cannot be expected. However, the reasonable agreement among the results shows the adequacy of the proposed approximate model.

Table 1. Resonance frequencies obtained from simulation and approximated analytical model

Structure	Resonance Frequency (Simulation)	Resonance Frequency (Analytical model)
Resonator (1)	6.1 GHz	5.5 GHz
Resonator (2)	8 GHz	7 GHz
Dual-Band Structure	6 GHz & 7.9 GHz	5.5 GHz & 7 GHz

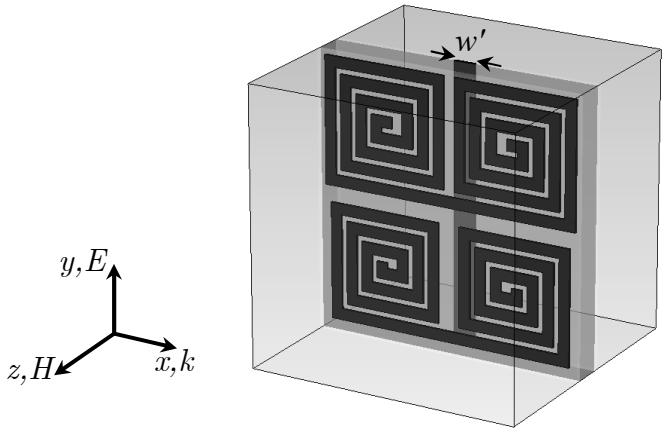

Figure 2. Schematic diagram of the proposed dual-band MTM structure unit cell with w' = 0.2 mm. The other geometric parameters are shown in Fig. 1.

3. Design of dual-band double negative metamaterial structure

In the preceding section a dual-band magnetic structure has been designed. In this section, the applicability of the proposed structure for designing dual-band double negative MTMs will be investigated. Figure 2 shows the layout of unit cell of the proposed MTM structure. The geometric dimensions are shown in Fig. 1. The use of proposed dual-band magnetic structure with a copper strip of width w' = 0.2 mm on the other side of dielectric board, produces a dual-band double negative MTM structure.

The electromagnetic properties of the proposed structure are obtained by numerical simulations, in a frequency range of 2 to 10 GHz by using CST Microwave Studio. The PEC and PMC boundary conditions are applied to the y and z directions and the absorbing boundary conditions are used in the x direction. The simulation results of transmission (S_{21}) and reflection (S_{11}) coefficients in a frequency range of 4 to 9 GHz are illustrated in Fig. 3(a). It can be easily shown that the impedance and refractive index of the MTM slab are given by:

$$z = \pm\sqrt{\frac{\left(1+S_{11}\right)^2 - S_{21}^2}{\left(1-S_{11}\right)^2 - S_{21}^2}} \tag{10}$$

$$n = \frac{i}{k_0 d}\ln\left[\frac{1}{S_{21}}\left(1-\frac{z-1}{z+1}S_{11}\right)\right] \tag{11}$$

The sign of square root in Eq. (10) should be chosen according to the energy conversation principle by the fact that the real part of z is positive. Since complex logarithmic function is a multi-branch one, the refractive index cannot be uniquely determined using Eq. (11); and so, the branch selecting problem is the challenge of MTM structures. It is clear that the imaginary part of refractive index can be unambiguously determined using Eq. (11). Considering this fact, Kramers-Kronig relations [34]:

$$\mathrm{Re}\{n(\omega)\} = 1 + \frac{2}{\pi}P.V\int_0^\infty \frac{u\,\mathrm{Im}\{n(u)\}}{u^2-\omega^2}du \tag{12}$$

$$\mathrm{Im}\{n(\omega)\} = -\frac{2\omega}{\pi}P.V\int_0^\infty \frac{\mathrm{Re}\{n(u)\}-1}{u^2-\omega^2}du \tag{13}$$

which connect the real and imaginary parts of the refractive index based on the causality principle were applied for solving the branch selecting problem [35]. In the above equations, P.V refers to the principal value of integral. However, in simulations and experiments, S-parameters are measured in limited frequency ranges, so the integrations of Eqs. (12) and (13) should be truncated. Also, it is noticed that upper limit of integration should be truncated at a frequency at which effective medium definition is valid. Thus, these relations yield only an approximation of real and imaginary parts of n. Thus, the proper

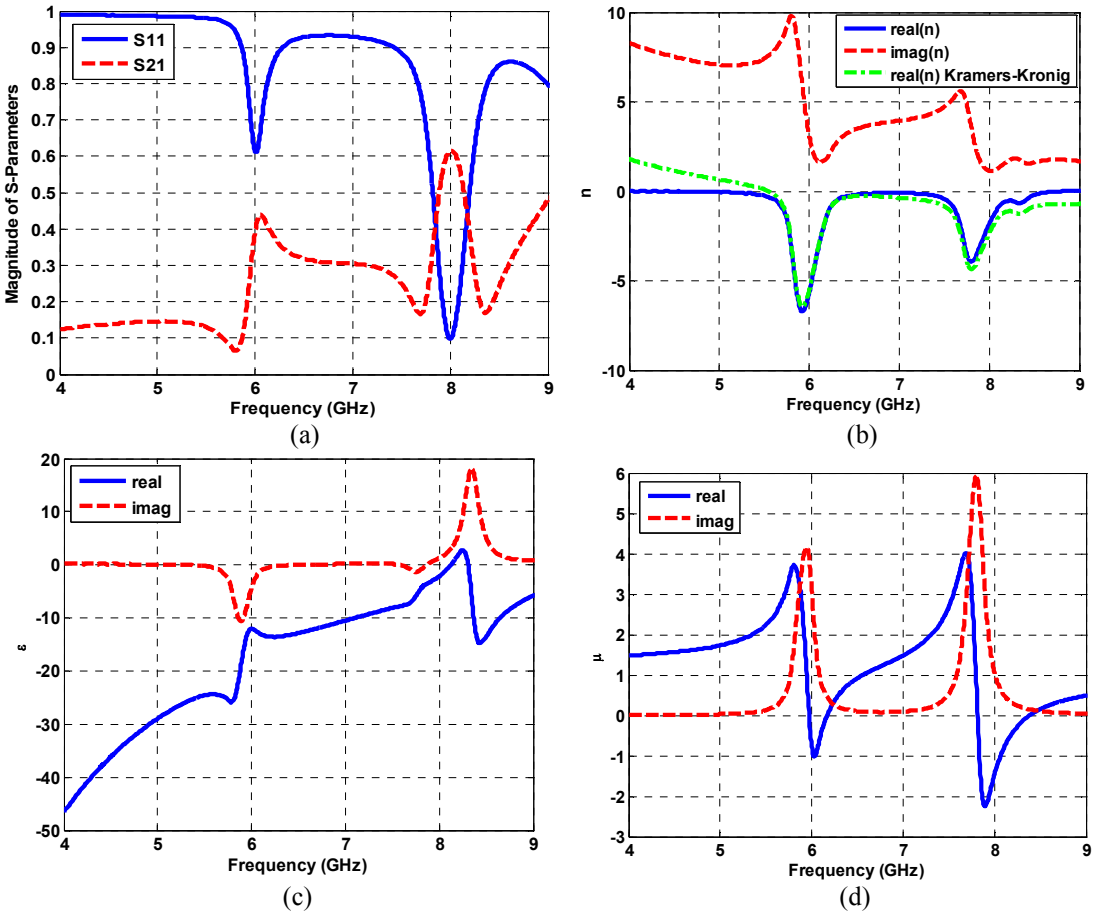

Figure 3. (a) Simulation results of the transmissions and reflection spectra, (b) refractive index, (c) real part of permittivity, and (d) real part of permeability of the proposed dual-band MTM structure.

branch can be selected such that the result of Eq. (11) is the closest to the K-K solution. Once z and n are unambiguously determined, effective permittivity and permeability of the structure could be identified subsequently, $\varepsilon = n/z$ and $\mu = nz$. The effective electromagnetic parameters of the proposed structure are retrieved and illustrated in Figs. 3(b)-3(d).

Note that, the first negative refraction region is around 6 GHz which is due to the upper symmetric spiral resonator. Besides, the second region is around 8 G which is due to the lower symmetric spiral resonator. The figure of merit FoM = |Re(n) / Im(n)|, is relatively low compared to the well-known single-band negative index material designs such as introduced structure in [27]. Simulations shows that the loss mainly originates from the lossy dielectric substrate which limits applicable frequency bands of NRI is due to the high loss of this MTM design. If low loss dielectric materials are used in the proposed design, the FoM can improve significantly. For instance, in our numerical simulations whose results are shown in Fig. 4, we obtained very high FoM (larger than 50) using a dielectric board with relative permittivity of 4.4 and loss tangent of 0.001.

The proposed dual-band MTM structure can be scaled to other frequencies and is also suitable for planar fabrication. In addition, as the significant advantage of the proposed structure, its dimensions are similar to that of well-known single-band MTM structure previously reported. The proposed structures may have many potential applications such as in dual-band antenna, dual-band focusing, dual-band filters, and dual-band microwave absorbers.

4. Conclusions

Symmetric spiral resonators were proposed and investigated to design dual-band artificial magnetic materials and double negative MTM structures. Also, an approximate analytical model was introduced for the initial design of dual-band artificial magnetic structures. Furthermore, the usefulness of the proposed structure for designing dual-band double negative MTMs was shown. The proposed structure has two NRI regions around 6 GHz and 8 GHz, which may be scaled to other frequencies. It seems that the

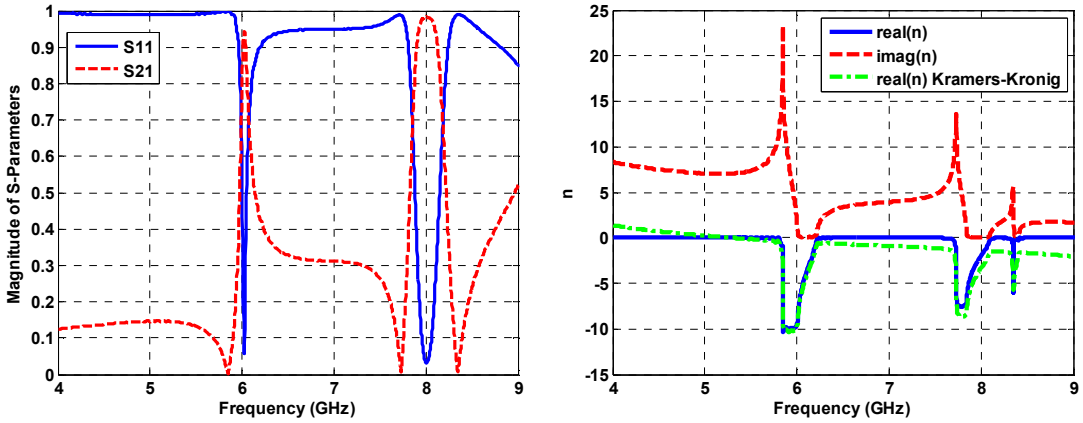

(a) (b)

Figure 4. (a) Simulation results of the transmissions and reflection spectra, (b) refractive index of the proposed dual-band MTM structure with low loss substrate.

proposed dual-band MTM structure which has unit cell dimensions similar to the well-known single-band microwave MTM structures can be used for improving the properties of dual-band antennas, filters, phase shifters, absorbers, and other microwave devices.

References

[1]. V.G. Veselago, The electrodynamics of substances with simultaneously negative values of ε and μ, Sov. Phys. Usp.10 (1968) 509-514.

[2]. D.R. Smith, W.J. Padilla, D.C. Vier, S.C. Nemat-Nasser, S. Schultz, Composite medium with simultaneously negative permeability and permittivity, Phys. Rev. Lett. 84 (2000) 4184-4187.

[3]. J. Zhou, L. Zhang, G. Tuttle, Th. Koschny, C.M. Soukoulis, Negative index materials using simple short wire pairs, Phys. Rev. B 73 (2006) 041101.

[4]. J. Zhou, L. Zhang, G. Tuttle, Th. Koschny, C.M. Soukoulis, Experimental demonstration of negative of index of refraction, Appl. Phys. Lett. 88 (2006) 221103.

[5]. Z.G. Dong, S.Y. Lei, Q. Li, M.X. Xu, H. Liu, T. Li, F.M. Wang, S.N. Zhu, Non-left-handed transmission and bianisotropic effect in a π-shaped metallic metamaterial, Phys. Rev. B 75 (2007) 075117.

[6]. G. Singh, Double Negative Left-Handed Metamaterials for Miniaturization of Rectangular Microstrip Antenna, J. Electromag. Analysis Appl. 2 (2010) 347-351.

[7]. H. Zhou, Z. Pei, S. Qu, S. Zhang, J. Wang, Q. Li, Z. Xu, A planar zero-index metamaterial for directive emission, J. Electromag. Waves Appl. 23 (2009) 953-962.

[8]. H. Attia, L. Yousefi, M. S. Boybay, O. M. Ramahi, Enhanced-Gain Microstrip Antenna Using Engineered Magnetic Superstrates, IEEE Antennas Propag. Lett. 8 (2009) 1198-1201.

[9]. B.I. Wu, , W. Wang, J. Pacheco, X. Chen, T. Grzegorczyk, J.A. Kong, A Study of Using Metamaterials as Antenna Substrate to Enhance Gain, Prog. Electromag. Res. 51 (2005) 295-328.

[10].B.-N. Zhang, T.-B. Yu, A.J. Liu, S.-J. Zhao, D.-S. Guo, Z.-D. Song, Single-feed dual-band dual-mode and dual-polarized microstrip antenna based on metamaterial structure, J. Electromag. Waves Appl. 25 (2011) 1909-1919.

[11].H. Zhou, S. Qu, Z. Pei, Y. Yang, J. Zhang, J. Wang, H. Ma, C. Gu, X. Wang, Z. Xu, W. Peng, P. Bai, A high-directive patch antenna based on all-dielectric near-zero-index metamaterial superstrates, J. Electromag. Waves Appl. 24 (2010) 1387-1396.

[12].J. B. Pendry, Negative refraction makes a perfect lens, Phys. Rev. Lett. 85 (2000) 3966-3969.

[13].Y. Zhang, R. Mittra, W. Hong, On the synthesis of a flat lens using a wideband low-reflection gradient index metamaterials, J. Electromag. Waves Appl. 25 (2011) 2178-2187.

[14].J. Bonache, I. Gil, J. Garcia-Garcia, F. Martin, Novel microstrip bandpass filters based on complementary split-ring resonators, IEEE Trans. Microw. Theory Tech. (2006).

[15].D. Li, Y. Xie, J. Zhang, J. Li, Z. Chen, "Multilayer filters with split-ring resonators," J. Electromag. Waves Appl. 22 (2008) 1420-1429.

[16].M. Naghshavarian Jahromi, Novel compact metamaterial tunable quasi elliptic band-pass filter microstrip to slotline transition, J. Electromag. Waves Appl. 24 (2010) 2371-2382.

[17].O. M. H. Ahmad, A.R. Sebak, Experimental investigation of new ultra wideband in-phase and quadrature-phase power splitter, J. Electromag. Waves Appl. 23 (2009) 2261-2270.
[18].L. Huang, H. Chen, Multi-band and polarization insensitive metamaterial absorber, Prog. Electromag. Res. 113 (2011) 103-110.
[19].X.-J. He, Y. Wang, J.-M. Wang, T.L. Gui, Dual-band terahertz metamaterial absorber with polarization insensitivity and wide incident angle, Prog. Electromag. Res. 115 (2011), 381-397.
[20].R. Mirzavand, B. Honarbakhsh, A. Abdipour, A. Tavakoli, Metamaterial-based phase shifters for ultra-wideband applications, J. Electromag. Waves Appl. 23 (2009) 1489-1496.
[21].R. Keshavarz, M. Movahhedi, A. Hakimi, A. abdipour, A novel broad bandwidth and compact backward coupler with high coupling level, J. Electromag. Waves Appl. 25 (2011) 283-293.
[22].S. Tretyakov, I. Nefedov, A. Sihvola, S. Maslovski, C. Simovski, Waves and energy in chiral nihility, J. Electromag. Waves Appl. 17 (2003) 695-706.
[23].J. Zhou, J. Dong, B. Wang, T. Koschny, M. Kafesaki, C.M. Soukoulis, Negative refractive index due to chirality, Phys. Rev. B 79 (2009) 121104.
[24].J. Zhou, J. Dong, B. Wang, T. Koschny, M. Kafesaki, C.M. Soukoulis, Negative refractive index due to chirality, Phys. Rev. B 79 (2009) 121104.
[25].R. Zhao, , L. Zhang, J. Zhou, T. Koschny, and C.M. Soukoulis, Conjugated gammadion chiral metamaterial with uniaxial optical activity and negative refractive index, Phys. Rev. B 83 (2011) 035105.
[26].D. Zarifi, , M. Soleimani, V. Nayyeri, A novel dual-band chiral metamaterials structure with giant optical activity and negative refraction index, J. Electromag. Waves Appl. 26 (2012) 251-263.
[27].D.R. Smith, D.C. Vier, Th. Koschny, C.M. Soukoulis, Electromagnetic parameter retrieval from inhomogeneous metamaterials, Phys. Rev. E 71 (2005) 036617.
[28].Y. Yuan, C. Bingham, T. Tyler, Dual-band planar electric metamaterial in the terahertz regime, Opt. Exp. 16 (2008) 9746-9752.
[29].E. Ekmekci, K. Topalli, T. Akin, G.T. Sayan, A tunable multi-band metamaterial design using micro-split SRR structures, Opt. Exp. 17 (2009) 16046-16058.
[30].M. Naghipourfar, Z. Atlasbaf, New dual-band DNG metamaterial, Canadian J. Electrical and Electronics Eng. 2 (2011) 47-56.
[31].S. Maslovski, P. Ikonen, I. Kolmakov, S. Tretyakov, Artificial magnetic materials based on the new magnetic particle: Metasolenoid, Progress Prog. Electromag. Res. 54 (2005) 61-81.
[32].L. Yousefi, O.M. Ramahi, Artificial magnetic materials using fractal Hilbert curves, IEEE Trans. Antenna Propag., 58 (2010) 2614-2622.
[33]. I. Bahl, P. Bhartia, Microwave Solid State Circuit Design, Wiley, New York, 1988.
[34].V. Lucarini, J. J. Saarinen, K.-E. Peiponen, and E. M. Vartiainen, Kramers-Kronig relations in Optical Maerials Research, Springer, Berlin Heidelberg, 2005.
[35].Z. Szabó G.-H. Park, R. Hedge, E.-P. Li, A unique extraction of metamaterial parameters based on the Kramers-Kronig relationships, IEEE Trans. Microwave Techniques 58 (2010) 2646-2653.